Shock Tube Studies Using a Novel Multipass Absorption Cell: Rate Constant Results For $OH + H_2$ and $OH + C_2H_6$

L. N. Krasnoperov[†] and J. V. Michael*[,‡]

Department of Chemistry and Environmental Science, New Jersey Institute of Technology, University Heights, Newark, New Jersey 07102, and Chemistry Division, Argonne National Laboratory, Argonne, Illinois 60439

Received: February 27, 2004; In Final Form: April 13, 2004

The reflected shock tube technique with a novel multipass absorption spectrometric detection method has been used to study two OH-radical reactions: $OH + H_2 \rightarrow H_2O + H$ (1), and $OH + C_2H_6 \rightarrow H_2O + C_2H_5$ (2). Reaction 1 was chosen in order to test the method against earlier rate constant determinations. The measurements on both reactions were performed in single-shot experiments with low initial concentrations of hydroxyl radicals, $[OH]_0 = (5-15) \times 10^{12}$ molecule cm^{-3}, which allowed reliable isolation of the elementary reactions. The measured rate constants are: $k_1 = 5.44 \times 10^{-11} \exp(-3220\ K/T)$ (832−1359 K), and $k_2 = 1.10 \times 10^{-10} \exp(-2537\ K/T)$ (822−1367 K), both in cm^3 molecule^{-1} s^{-1}. The present study extends the experimental T-range for reaction 2. This new work and earlier lower-T studies have been combined to give a new evaluation, $k_2 = 2.68 \times 10^{-18}\ (T/K)^{2.224} \exp(-373\ K/T)$ cm^3 molecule^{-1} s^{-1}. An ab initio potential energy surface was additionally used to derive a theoretical expression for this reaction.

Introduction

Reliable determinations of rate constants for elementary free-radical chemical reactions require reaction isolation; i.e., reduction of the contributions of undesirable radical−radical and radical−molecule reactions. Better isolation of an elementary reaction generally requires low initial concentrations of free-radical species in order to reduce or eliminate the unwanted secondary reactions. Hence, improved sensitivity for detection is then required. A high-temperature shock-tube experiment, being a single-shot experiment, presents the worst situation because signal accumulation techniques are either impossible or very limited.

In the current study, a novel multipass absorption technique has been evaluated for sensitive time-resolved monitoring in shock-tube experiments. The technique has been used to monitor OH-radical concentrations at 308 nm in reflected shock tube experiments. The technique has been evaluated by measuring rate constants for two elementary reactions of OH:

$$OH + H_2 \rightarrow H_2O + H \quad (1)$$

$$OH + C_2H_6 \rightarrow H_2O + C_2H_5 \quad (2)$$

The rate behavior for the first reaction is well known, and therefore the method can be tested by comparing the experimental results for reaction 1 to earlier studies.

Experimental Section

The present experiments were performed with the reflected shock tube technique and OH-radical detection using absorption of the electronic transition in the near-UV. The basics of the shock tube method and the apparatus have been previously described,[1,2] and only a brief description of the experiment will be presented here.

The apparatus consists of a 7-m (4-in. o.d.) 304 stainless steel tube separated from the He driver chamber by a 4-mil unscored 1100-H18 aluminum diaphragm. The tube was routinely pumped between experiments to $<10^{-8}$ Torr by an Edwards Vacuum Products model CR100P packaged pumping system. The velocity of the shock wave was measured with eight equally spaced pressure transducers (PCB Piezotronics, Inc., model 113A21) mounted along the end portion of the shock tube, and temperature and density in the reflected shock wave regime were calculated from this velocity and include corrections for boundary layer perturbations.[3−5] A 4094C Nicolet digital oscilloscope was used to record velocity gauge signals, and an LC334A LeCroy digital oscilloscope was used to record the absorption signals. Delayed pulses that derive from the last velocity gauge signal triggered both oscilloscopes.

In the current experiments we used an OH resonance lamp.[6,7] High sensitivity in the transient absorption measurements was achieved with a multipass cell of a novel design. A detailed description of the cell and the theory of operation are given elsewhere.[8] Briefly, the cell is an optically stable Fabry-Perot cavity consisting of high reflectivity (at the detection wavelength, around 308 nm) planar and spherical concave mirrors. The mirrors were installed outside the shock tube. The tube was equipped with two flush fused silica windows with broadband antireflection (BB AR) coatings on both sides. The path length inside the tube was 8.745 cm. The monitoring light source (MW discharge driven OH lamp) was placed at a distance of 20 cm from the cell. The monitoring light was collimated onto the multipass cell using a fused silica lens ($f = 9.6$ cm). The concave dielectric mirror has a 20 cm radius of curvature. The manufacturer stated reflectivity for both mirrors was 98.0 ± 1.0% at 308 nm. Actual transmittances of the mirrors (as determined in separate measurements) were 2.90% for the planar and 2.33% for the concave mirrors. The mirrors were mounted in angular adjustable mounts at a distance of 14.5 cm. With

* Corresponding Author: Dr. J. V. Michael D-193, Bldg. 200 Argonne National Laboratory Argonne, IL 60439. Phone: (630) 252-3171. Fax: (630) 252-4470. E-mail: jmichael@anl.gov.
[†] New Jersey Institute of Technology.
[‡] Argonne National Laboratory.

10.1021/jp040186e CCC: $27.50
Published on Web 06/08/2004

this geometry the mirrors form an optically stable Fabry−Perot cavity (stable in the sense that an optical ray under the approximation of the geometrical optics will never leave the cavity). The increase in the sensitivity is achieved due to multiple reflections of the monitoring light inside the cell. A simple theory[8] implies that the "gain", *G*, of the cell (the average number of passes of a photon inside the cell) is given by

$$G = \text{OnePassLoss}^{-1} \qquad \text{(E1)}$$

where OnePassLoss is the one pass loss of the cavity at the monitoring wavelength.

Equation E1 predicts a maximum expected theoretical gain of 38 based on the mirrors' *transmissions*. The actual gain is lower due to mirror absorption, to losses in the windows, and to the imperfect coupling of the monitoring beam with the cavity (see ref 8, Appendix). The actual gain of the cell was determined using absorption of the monitoring light by a stable compound, acetone. The cross-section of acetone was measured in a single-pass arrangement using the same light source (MW discharge OH resonance lamp), giving σ(acetone, 296 K) = (1.492 ± 0.022) × 10^{-20} cm^2 $molecule^{-1}$. The cell calibration and the gain stability were routinely checked, and the measured cell gain ($G = 12.4 \pm 1.0$) was stable within the quoted uncertainty for all of the reported experiments.

Monitoring light emerging from the cell was focused using a fused silica lens ($f = 9.6$ cm) onto a photocathode of a photomultiplier tube through a narrow-band interference filter (Oriel, central wavelength 308.2 nm, fwhm = 8.6 nm). The mirrors, lenses, and windows were obtained from the CVI Laser Corporation.

A small fraction of the monitoring light emerging from the lamp was split by a thin fused silica plate and directed to a reference PMT through an identical narrow-band interference filter. The signal from this PMT was recorded in the second channel of the digital oscilloscope. Weighted reference signal was subtracted from the signal of the first photomultiplier to substantially reduce the light intensity fluctuations caused by power supply residual line frequency ripple as well as by the plasma instabilities within the lamp.

MW Discharge Driven Resonance OH Lamp. The MW driven resonance lamp was made from 6 mm OD fused silica tubing. The discharge was driven by a microwave power supply (2.45 GHz, Opthos, Inc.) using an Evenson type MW cavity (Opthos, Inc.). The cavity was cooled by compressed air flow. A flow of argon at 1.28 ± 0.07 bar and 296 K was saturated with water vapor and then pumped through a needle valve into the lamp in the direction opposite to the emitted light. The empirically found optimum conditions for the lamp operation were with the total gas pressure equal to ∼25 Torr. We added two 1 L buffer flasks before and after the lamp to reduce the pressure pulsations caused by the mechanical pump and the Ar cylinder pressure regulator. The discharge power was 70 W, with the reflected power below 1 W. The apparent absorption cross-section of hydroxyl radical, measured in this work, refers to these operational conditions. The spectrum of the lamp was evaluated using a grating spectrograph (Acton Research Corp. VM 502, 600 1/mm, 2nd order). When recorded with low resolution of 0.25 nm, the spectrum consists of ∼17 lines between 308 and 320 nm, and 90% of the total intensity is concentrated in 11 "lines" located between 308 and 316 nm.

Gases. High purity He (99.995%), used as the driver gas, was from AGA Gases. Scientific grade Kr (99.999%), the diluent gas in reactant mixtures, was from Spectra Gases, Inc. The ∼10 ppm impurities (N_2, 2 ppm; O_2, 0.5 ppm; Ar, 2 ppm; CO_2, 0.5 ppm; H_2, 0.5 ppm; CH_4, 0.5 ppm; H_2O, 0.5 ppm; Xe, 5 ppm; and CF_4, 0.5 ppm) are all either inert or in sufficiently low concentration so as to not perturb OH-radical profiles. Distilled water, evaporated at ∼1 bar into ultrahigh purity grade Ar (99.999%) from AGA Gases, was used at ∼25 Torr pressure in the resonance lamp. Analytical grade C_2H_5I (99%) from Aldrich Chemical Co. Inc., and technical grade NO_2 from Matheson Gas Products were both further purified by bulb-to-bulb distillation with the middle thirds being retained. 90% tertiary butyl hydroperoxide (*tert*-butyl HP) was obtained from Sigma Aldrich Chemical Co. and was used as received. This compound is unstable, and, therefore, an NMR analysis was carried out giving an actual purity level of 71%. Scientific grade H_2 (99.9999%) was obtained from MG Industries and was used without additional purification. Research grade C_2H_6 (99.95%) was obtained from AGA Gases and was purified by bulb-to-bulb distillation, retaining only the middle third. Purified HNO_3 was prepared and cold stored as a distillate from fuming nitric acid and concentrated sulfuric acid. Test gas mixtures were accurately prepared from pressure measurements using a Baratron capacitance manometer and were stored in an all glass vacuum line.

Results and Discussion

Performance of the Multipass Cell in the Shock-Tube Environment. We had two concerns about the performance of the multipass cell in the high temperature shock tube environment, the first being whether the cell gain would be significantly reduced because of window contamination or deterioration. Inexpensive windows were therefore mounted directly on the shock tube even though using these BB AR coated windows reduces the cell gain.[8] The alternative would have been to directly mount the expensive mirrors on the shock tube. With AR windows on the tube and mirrors mounted externally, we found no changes in the cell gain even with long-term operation. Hence, deterioration of performance is negligible, and this observation suggests that if the cell mirrors were directly installed on the shock tube then the sensitivity of the cell could be significantly increased.

Our second concern was whether the rapid density increases in both incident and reflected shock waves would affect the index of refraction (Schlieren effects), thereby substantially changing the light intensity. However, it was observed that this multipass cell design is much less susceptible to Schlieren effects than the cells of traditional design. Changes in the index of refraction lead to the beam deflection, which, in traditional designs, leads to light intensity modulation at the cell apertures. In the current design, due to the optical stability of the cell, deflected photons do not lead to the intensity variations because deflected photons are still confined to the optical cavity. The experimental traces show that incident but also reflected shock waves are barely visible. This observation suggests that a further increase in the sensitivity using higher reflectivity mirrors installed directly on the shock tube would be a significant advance and could be carried out without Schlieren interference.

Apparent Absorption Cross-Section and the Self-Reaction of OH Radicals. The apparent absorption cross-sections for OH-radicals with the MW discharge lamp described above was measured using the single-pass arrangement. This necessitated measuring the OH-radical absorption coefficient under conditions similar to the kinetics experiments. Using C_2H_5I/NO_2 mixtures, the ethyl radicals formed from the dissociation of ethyl-iodide subsequently decompose, giving $H + C_2H_4$ (reaction 3a below).[9] The H-atoms then react with NO_2 giving OH

+ NO[7] (reaction 4 below). This method has been described,[6,7] and, in this work, absorption coefficients for OH-radicals were measured over the temperature range 1116−1875 K.

The major reactions are

$$C_2H_5I\ (+\ M) \rightarrow C_2H_5 + I\ +(M) \rightarrow C_2H_4 + H + I\ +(M) \quad (3a)$$

$$\rightarrow C_2H_4 + HI\ +(M) \quad (3b)$$

$$H + NO_2 \rightarrow OH + NO \quad (4)$$

$$OH + OH \rightarrow H_2O + O \quad (5)$$

$$O + C_2H_4 \rightarrow C_2H_3 + OH \quad (6)$$

$$C_2H_3\ (+M) \rightarrow C_2H_2 + H\ (+M) \quad (7)$$

The main feature of this mechanism is that two OH radicals consumed in the self-reaction are returned in the subsequent reactions of O atoms with ethylene in reaction 6, followed by 7 and 4. This feature simplifies the single-pass measurements of OH absorption by prolonging the lifetime of OH radicals; however, it simultaneously makes measurements of the self-reaction of OH radicals, reaction 5, impossible using this generator for OH.

Temporal profiles of OH absorption in the pyrolysis of $C_2H_5I/NO_2/Kr$ mixtures were acquired over the temperature range 1116−1875 K. The profiles were fitted using an extended reaction mechanism, with reactions 3−7 being the major ones. The branching ratio in the dissociation of ethyl iodide, reaction 3, is $f_{3a} = 0.85$.[9] The resultant data were fitted using linear regression giving

$$\sigma_{app}(OH) = ((4.16 \pm 0.40) - (1.05 \pm 0.26)\ (T/1000\ K)) \times 10^{-17}\ cm^2\ molecule^{-1} \quad (E2)$$

This compares well with previous studies[6] where a multiline source of OH radiation has been used.

Some experiments were performed with single pass optics to measure the self-reaction of OH radicals, k_5. As already mentioned above, the chemical system, reactions 3−7, used to measure absorption cross-sections for OH, is not suitable for measuring k_5. Instead, OH radicals were formed from the thermal decomposition of HNO_3. In agreement with earlier work,[10] we found that we could deliver concentrations of 45−65% HNO_3 from fresh mixtures in passivated storage bulbs. Three experiments were performed at 1504, 1545, and 1547 K giving 5.2, 4.7, and 4.6 × 10^{-12} cm^3 $molecule^{-1}$ s^{-1}, respectively. These values agree with those of Wooldridge et al.[10] within experimental error.

Reaction OH + H_2. To measure rate constants for the reaction of OH with molecular hydrogen, reaction 1, multipass absorption experiments were performed. In this case, OH radicals were prepared from the thermal decomposition of *tert*-butyl hydroperoxide, $(CH_3)_3COOH$, giving $(CH_3)_2CO$, OH, and CH_3. *tert*-Butyl hydroperoxide has been used previously[11] for OH preparation. This molecule is so unstable that it decomposes almost instantaneously above ∼800 K,[12] thereby limiting the temperature range in the present reflected shock wave experiments to <1370 K. In the earlier work,[11] several rate constants for OH with H_2 and three hydrocarbon molecules were measured at 1200 K, using single-pass absorption. Decay constants were determined as a function of added reactant concentration, $[R]_0$, and the slopes of linear plots gave the rate constants. This procedure assumes that secondary reaction contributions are unchanged from the case with no added reactant to finite reactant concentration, an assumption that is not necessarily correct. In the present experiments, we include the effects of secondary reactions by using them for profile fitting in chemical simulations with k_1 being the unknown rate constant. Experiments with $[OH]_0 \leq 2 \times 10^{13}$ molecules cm^{-3} have been carried out, and a typical temporal profile of OH absorption is shown in Figure 1. While an extended mechanism was used to fit the data, only a few secondary reactions play a significant role at this relatively low $[OH]_0$. The decay of OH in these experiments is dominated by reaction with H_2. The relative role of other reactions in these experiments is apparent from Figure 1, where the dashed line represents a simulation of the decay with reaction 1 turned off. Typically, the contribution of the other reactions in the mechanism to the decay of OH radicals was 10−15%. The mechanism includes *tert*-butyl hydroperoxide decomposition,[12] CH_3-radical recombination,[13] OH-radical recombination,[10] CH_3- and OH-radical cross-combination,[14] and several other reactions of minor importance. In addition, we have fitted OH profiles in the absence of H_2 and have estimated CH_3 + OH. These are well within a factor of 2 of the temperature-extrapolated results from Pereira et al.[14] With added H_2, reaction 1 becomes by far the dominant removal process for OH, and, therefore, confident values for k_1 can be extracted from profile fits. An example of a simulated least squares profile fit (solid thin line) to an experimental record is shown in Figure 1. The experimental conditions and measured values for k_1 are summarized in Table 1, and the Arrhenius plot for k_1 is shown in Figure 2. The present data can be expressed in Arrhenius form as

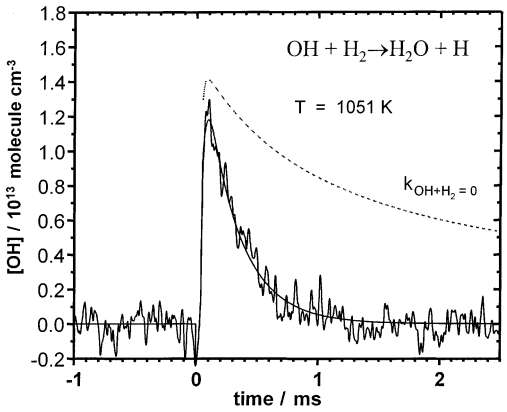

Figure 1. Sample temporal profile of OH absorption for an OH + H_2 experiment with P_1 = 20.88 Torr, M_s = 2.020, $\rho_5 = 3.091 \times 10^{18}$ molecules cm^{-3}, T_5 = 1051 K, $[H_2]_0 = 1.250 \times 10^{15}$ molecules cm^{-3}, and [*tert*-butyl HP]$_0 = 1.62 \times 10^{13}$ molecules cm^{-3}. The solid line through the experimental profile is the nonlinear least-squares fit to the data with the reaction mechanism (see text). The value returned by the fit for k_1 is 2.44 × 10^{-12} cm^3 $molecule^{-1}$ s^{-1}. The dashed line is a simulation with the same mechanism but with $k_1 = 0$.

$$k_1 = 5.44 \times 10^{-11} \exp(-3220\ K/T) \quad (E3)$$

over the temperature range, 832−1359 K.

Earlier k_1 measurements are extensive.[12] Quite accurate direct measurements and subsequent evaluations over an extended temperature range are available, and the rate behavior can be summarized by the three-parameter expression[1,15]

$$k_1 = 3.56 \times 10^{-16}\ (T/K)^{1.52} \exp(-1736\ K/T) \quad (E4)$$

in molecular units for 250−2580 K. This expression is plotted in Figure 2 along with the present data and eq E3. Over the present T-range, eq E3 is only ∼10% lower than values from

TABLE 1: High Temperature Rate Data for OH + H_2 → H + H_2O ($X_{t-butyl\ HP} = 5.243 \times 10^{-6}$, $X_{H_2} = 4.044 \times 10^{-4}$)

P_1/Torr	M_s[a]	$\rho_5/(10^{18}$ cm$^{-3})$[b]	T_5/K[b]	$k_1/1 \times 10^{-12}$ [c]
10.91	2.096	1.716	1138	3.54 ± 0.15[d]
10.97	1.951	1.567	1001	2.34 ± 0.12
10.94	2.178	1.803	1219	4.19 ± 0.27
10.93	1.756	1.333	832	1.06 ± 0.07
10.94	1.990	1.606	1037	2.75 ± 0.15
10.92	2.314	1.930	1359	5.48 ± 0.47
10.91	1.936	1.542	988	1.61 ± 0.08
10.89	1.830	1.416	894	2.10 ± 0.15
20.93	2.230	3.299	1148	3.23 ± 0.12
20.99	2.077	3.219	1103	2.18 ± 0.11
20.88	2.020	3.091	1051	2.44 ± 0.08
20.99	1.913	2.888	956	1.90 ± 0.06
20.85	1.844	2.720	896	1.26 ± 0.05
20.83	2.313	3.618	1336	5.21 ± 0.33
20.88	2.289	3.586	1311	4.05 ± 0.25

[a] The error in measuring the Mach number, M_s, is typically 0.5−1.0% at the one standard deviation level. [b] Quantities with the subscript 5 refer to the thermodynamic state of the gas in the reflected shock region. [c] Rate constants in units cm^3 molecule^{-1} s^{-1}. [d] The errors shown are ±3 St. Dev. and reflect the statistical accuracy of the fits only.

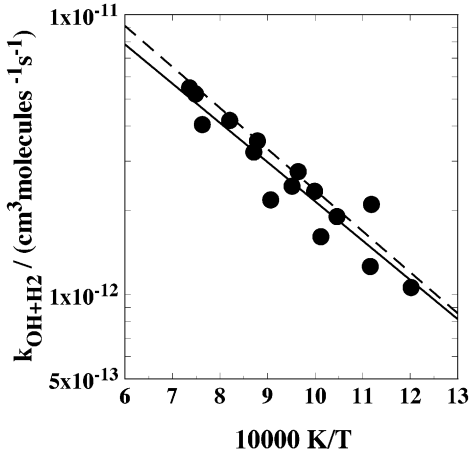

Figure 2. Arrhenius plot for OH + H_2. The solid line is the linear regression given in eq E3, and the dashed line is the evaluation described in the text, eq E4.

the evaluation, eq E4, showing that the present multipass method can be used to accurately measure OH rate constants.

Reaction OH + C_2H_6. Similar experiments have been carried out for OH + C_2H_6 → H_2O + C_2H_5. A sample absorption profile is shown in Figure 3. Again with the full mechanism, the solid line shows the nonlinear least-squares fit (with variable k_2) to the data, and the dashed line shows the decay with $k_2 = 0$. The decay is clearly dominated by the reaction, and the rate constant results are therefore direct. The data are summarized in Table 2, and an Arrhenius plot of the rate behavior is shown in Figure 4. The solid line in the figure is a linear-least-squares fit to the data giving the expression

$$k_2 = 1.10 \times 10^{-10} \exp(-2537\ \text{K/T}) \qquad \text{(E5)}$$

over the experimental temperature range 822−1367 K.

Even though the database on reaction 2 is extensive,[12,16] a close examination shows that there are only two fairly direct determinations at temperatures >950 K. Bott and Cohen[17] and Koffend and Cohen[18] report values of 1.49×10^{-11} and 8.39×10^{-12} cm^3 molecule^{-1} s^{-1} at 1200 and 970 K, respectively. Hence, the values in Table 2 are the first direct determinations for this reaction above 1200 K.

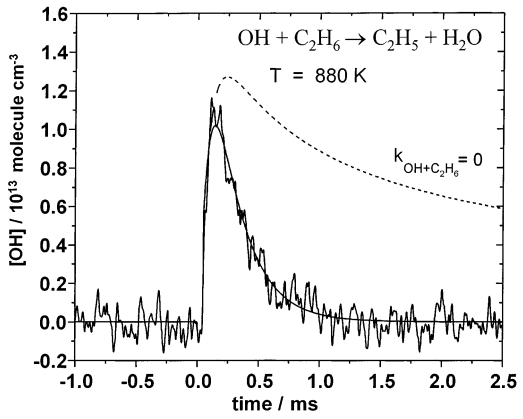

Figure 3. Sample temporal profile of OH absorption for an OH + C_2H_6 experiment with $P_1 = 20.90$ Torr, $M_s = 1.824$, $\rho_5 = 2.682 \times 10^{18}$ molecules cm^{-3}, $T_5 = 880$ K, $[C_2H_6]_0 = 4.452 \times 10^{14}$ molecules cm^{-3}, and [*tert*-butyl HP]$_0 = 1.460 \times 10^{13}$ molecules cm^{-3}. The solid line through the experimental points is the nonlinear least-squares fit to the data with the reaction mechanism (see text). The value for k_2 returned by the fit is 8.05×10^{-12} cm^3 molecule^{-1} s^{-1}. The dashed line is a simulation with the same mechanism, but with $k_2 = 0$.

TABLE 2: High Temperature Rate Data for OH + C_2H_6 → H_2O + C_2H_5 ($X_{t-butyl\ HP} = 5.445 \times 10^{-6}$, $X_{C_2H_6} = 1.660 \times 10^{-4}$)

P_1/Torr	M_s [a]	$\rho_5/(10^{18}$ cm$^{-3})$[b]	T_5/K[b]	$k_2/1 \times 10^{-12}$ [c]
10.90	2.134	1.758	1171	12.3 ± 0.9[d]
10.95	1.970	1.590	1016	6.24 ± 0.33
10.96	2.325	1.954	1367	19.7 ± 2.1
10.93	1.916	1.527	967	7.46 ± 0.40
10.86	1.822	1.408	885	4.64 ± 0.27
20.92	2.333	3.665	1357	16.7 ± 1.5
20.90	2.031	3.114	1061	9.68 ± 0.51
20.90	1.824	2.682	880	8.05 ± 0.42
20.79	1.754	2.512	822	6.34 ± 3.70
20.96	2.191	3.427	1213	15.5 ± 1.60

[a] The error in measuring the Mach number, M_s, is typically 0.5−1.0% at the one standard deviation level. [b] Quantities with the subscript 5 refer to the thermodynamic state of the gas in the reflected shock region. [c] Rate constants in units cm^3 molecule^{-1} s^{-1}. [d] The errors shown are ±3 St. Dev. and reflect the statistical accuracy of the fits only.

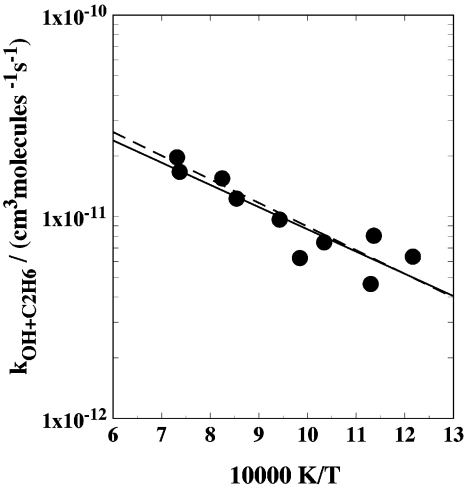

Figure 4. Arrhenius plot for OH + C_2H_6. The solid line is the linear regression given in eq E5 and the dashed line is the evaluation described in the text, eq E6.

Since approximately the year 1980, as documented in the NIST database,[12] there are about seven evaluations of the rate behavior for reaction 2 over the extended T-range, 300−2000 K. These evaluations have used a variety of data sources that

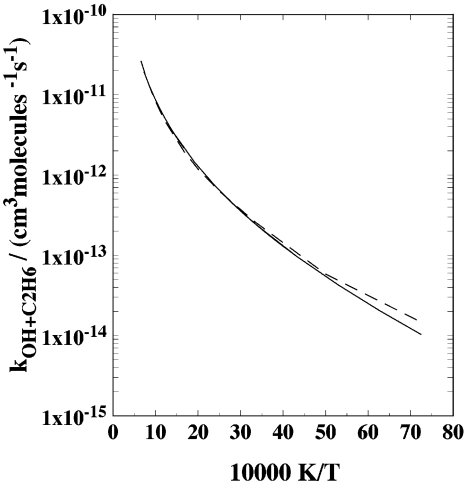

Figure 5. Comparison of theory to experiment for reaction 2: OH + C_2H_6 (—) experiment, eq E6; (– – –) theory, eq E7.

include direct lower-T determinations and inferences from mechanistic fitting of complex reacting systems such as those from flat flame burner studies.[19] Some of these evaluations[20] have also relied on theoretical methods as an aid for extrapolation of the rate constants beyond the T-range of experiment. As new data have become available, the T-dependent evaluations have changed. In addition to the present study, Tully et al.,[16] and Cohen and co-workers,[17,18] there have been four direct T-dependent studies during the past decade.[21−24] Since much of the data is recent, we have reevaluated the rate behavior for reaction 2 using our data and the aforementioned studies.[16−18,21−24] The T-range extends from 138 to 1367 K. We have constructed a database from these studies by evaluating rate constants from reported two- and three-parameter Arrhenius expressions. We used five points, equally spaced in T^{-1}, from each study, but only over the T-range of a given study. We included the individual points from the two studies by Cohen and co-workers. A three parameter nonlinear least squares modified Arrhenius expression was determined from the database giving, in molecular units,

$$k_2 = 2.68 \times 10^{-18} (T/K)^{2.224} \exp(-373\ K/T) \quad (E6)$$

This expression is plotted in Figures 4 and 5 over the T-ranges 822−1367 and 138−1367 K, respectively. If eq E6 is compared to the data points used to determine it, the points deviate from E6 by ±6.4% at the one standard deviation level. In fact, this equation gives values that are within ±13% for all studies with the exception of Sharkey and Smith,[21] where the maximum discrepancy is −26%. Over the full experimental T-range, we have also tested the accuracy of other evaluations against the data points. Cohen's expression[20] gives a one standard deviation discrepancy of ±14.5%, whereas the Tully et al.[16] and Baulch et al.[25] expressions give ±8.4% and ±9.0%, respectively. Hence, eq E6 is the superior representation for k_2 over a large T-range. It should additionally be noted that eq E6 predicts values in the 1500−1800 K range that are <8.6% higher than the inferences from the flame study.[19]

The evaluation by Cohen[20] involved theoretical extrapolation with the group additivity version of conventional transition state theory (CTST).[26] To fit the existing data, including the values from the two studies by Cohen and co-workers,[17,18] the barrier height had to be adjusted to 2424 cal mol^{-1}, and one of the low valued bends had to be taken as 250 cm^{-1}. With a simple approximate model derived from transition state theory, Donahue et al.[24] used doubly and singly degenerate bends, 500 and 300 cm^{-1}, respectively, to explain their data on OH + alkanes over a much narrower T-range. Surprisingly, there are no reports of CTST rate constant estimates using electronic structure calculations as a basis. We have used a B3LYP/6−31g* calculation[27] for structures and force fields for both ethane and the transition state (TS) to estimate the rate behavior over the T-range 140−1600 K. The CH_3-hindered rotors in ethane and TS were assumed to cancel, but the OH rotor was assumed to be free. Following Cohen,[20] the low lying bend was taken as 250 cm^{-1}, and Wigner tunneling corrections were included with the scaled imaginary frequency from the electronic structure calculation being 969i. For the best fit to eq E6, the barrier height was adjusted to the same value as used by Cohen; i.e., 2424 cal mol^{-1}. In molecular units, the theoretical calculation can be expressed to within <6% by the expression

$$k_2^{th} = 3.16 \times 10^{-19} (T/K)^{2.508} \exp(-223\ K/T) \quad (E7)$$

for $140 \le T \le 1600$ K. Equation E7 is compared to E6 in Figure 5 where it is seen that deviations occur at lower temperatures. Even though a CTST calculation can be made to approximately fit experiment, the present level of electronic structure calculation is not accurate. We therefore suggest that this reaction should be studied in the future with higher-level electronic structure methods.

Conclusions

In the present work we have described a novel multipass optical method for measuring OH-radical concentrations in reflected shock wave experiments. Three determinations of rate coefficients for OH + OH were reported. The multipass method was evaluated in a study of the OH + H_2 reaction, and the method was used to study the OH + C_2H_6 reaction at temperatures never before achieved. In all three cases, the results were compared to earlier studies. This direct method gives values that agree with earlier work and therefore offers a novel method for directly probing chemical reactivity in high-temperature experiments.

Acknowledgment. The authors thank Dr. L. B. Harding for supplying the B3LYP/6-31g* calculation for OH + C_2H_6. We also thank Drs. J. P. Hessler and N. K. Srinivasan for helpful discussions. This work was supported by the U.S. Department of Energy, Office of Basic Energy Sciences, Division of Chemical Sciences, Geosciences and Biosciences under Contract No. W-31-109-Eng-38.

References and Notes

(1) Michael, J. V. *Prog. Energy Combust. Sci.* **1992**, *18*, 327.
(2) Michael, J. V. In *Advances in Chemical Kinetics and Dynamics*; Barker, J. R., Ed.; JAI: Greenwich, 1992; Vol. I, pp 47−112, for original references.
(3) Michael, J. V.; Sutherland, J. W. *Int. J. Chem. Kinet.* **1986**, *18*, 409.
(4) Michael, J. V. *J. Chem. Phys.* **1989**, *90*, 189.
(5) Michael, J. V.; Fisher, J. R. In *Seventeenth International Symposium on Shock Waves and Shock Tubes*; AIP Conference Proceedings 208; Kim, Y. W., Ed.; American Institute of Physics: New York, 1990; pp 210−215.
(6) Su, M.-C.; Kumaran, S. S.; Lim, K. P.; Michael, J. V. *Rev. Sci. Instrum.* **1995**, *66*, 4649.
(7) Su, M.-C.; Kumaran, S. S.; Lim, K. P.; Michael, J. V.; Wagner, A. F.; Harding, L. B.; Fang, D.-C. *J. Phys. Chem. A* **2002**, *106*, 8261.
(8) Grebenkin, S. Yu.; Krasnoperov, L. N. *J. Phys. Chem. A* **2004**, *108*, 1953.
(9) Kumaran, S. S.; Su, M.-C.; Lim, K. P.; Michael, J. V. *Proc. Combust. Inst.* **1996**, *26*, 605.

(10) Wooldridge, M. S.; Hanson, R. K.; Bowman, C. T. *Int. J. Chem. Kinet.* **1994**, *26*, 389.
(11) Bott J. F.; Cohen, N. *Int. J. Chem. Kinet.* **1989**, *21*, 485.
(12) *NIST Chemical Kinetics Database*, NIST Standard Reference Database 17, Gaithersburg, MD, 2000.
(13) Walter, D.; Grotheer, H.-H.; Davies, J. W.; Pilling, M. J.; Wagner, A. F. *Proc. Combust. Inst.* **1990**, *23*, 107. (b) Hwang, S. M.; Rabinowitz, M. J.; Gardiner, W. C., Jr. *Chem. Phys. Lett.* **1993**, *205*, 157. (c) Davidson, D. F.; Di Rosa, M. D.; Chang, A. Y.; Hanson, R. K.; Bowman, C. T. *Proc. Combust. Inst.* **1992**, *24*, 589. (d) Davidson, D. F.; Hanson, R. K.; Bowman, C. T. *Int. J. Chem. Kinet.* **1995**, *27*, 305.
(14) De Avillez Pereira, R.; Baulch, D. L.; Pilling, M. J.; Robertson, S. H.; Zeng, G. *J. Phys. Chem. A* **1997**, *101*, 9681.
(15) Oldenborg, R. C.; Loge, G. W.; Harradine, D. M.; Winn, K. R. *J. Phys. Chem.* **1992**, *96*, 8426.
(16) Tully, F. P.; Droege, A. T.; Koszykowski, M. L.; Melius, C. F. *J. Phys. Chem.* **1986**, *90*, 691.
(17) Bott, J. F.; Cohen, N. *Int. J. Chem. Kinet.* **1991**, *23*, 1017.
(18) Koffend, I. B.; Cohen, N. *Int. J. Chem. Kinet.* **1996**, *28*, 79.
(19) Ancia, R.; Vandooren, J.; Van Tiggelen, P. J. *Proc. Symp. Combust.* **1996**, *26*, 1009.
(20) Cohen, N. *Int. J. Chem. Kinet.* **1991**, *23*, 397.
(21) Sharkey, P.; Smith, I. W. M. *J. Chem. Soc., Faraday Trans.* **1993**, *89*, 631.
(22) Talukdar, R. K.; Melouki, A.; Gierczak, T.; Barone, S.; Chiang, S.-Y.; Ravishankara, R. *Int. J. Chem. Kinet.* **1994**, *26*, 973.
(23) Crowley, J. N.; Campuzano-Jost, P.; Moortgat, G. K. *J. Phys. Chem.* **1996**, *100*, 3601.
(24) Donahue, N. M.; Anderson, J. G.; Demerjian, K. J. *J. Phys. Chem. A* **1998**, *102*, 3121.
(25) Baulch, D. L.; Cobos, C. J.; Cox, R. A.; Esser, C.; Frank, P.; Just, Th.; Kerr, J. A.; Pilling, M. J.; Troe, J.; Walker, R. W.; Warnatz, J. *J. Phys. Chem. Ref. Data* **1992**, *21*, 411.
(26) Benson, S. W. *Thermochemical Kinetics*, 2nd ed.; Wiley: New York, 1976.
(27) Harding, L. B., private communication, Feb., 2004.